

Optimization Studies on Imatinib Mesylate Loaded Nanoliposomes Using Box-Behnken Design

Mandeep Dahiya^{1#}, Rajendra Awasthi^{2#}, Gaurav Gupta³, Sachin Kumar Singh⁴, Monica Gulati⁴, Niraj Kumar Jha⁵, Saurabh Kumar Jha⁵, Ankur Sharma⁶, Parteek Prasher⁷, Krishnan Anand⁸, Dinesh Kumar Chellappan⁹, Kamal Dua¹⁰, Harish Dureja^{1✉}

¹Department of Pharmaceutical Sciences, Maharshi Dayanand University, Rohtak, 124001, India.

²Amity Institute of Pharmacy, Amity University Uttar Pradesh, Noida, 201313, India.

³School of Pharmaceutical Sciences, Suresh Gyan Vihar University, Jaipur, Rajasthan, India.

⁴School of Pharmaceutical Sciences, Lovely Professional University, Phagwara, 144411, Punjab, India.

⁵Department of Biotechnology, School of Engineering and Technology (SET), Sharda University, Uttar Pradesh, Noida, 201301, India.

⁶Department of Life Sciences, School of Basic Science and Research (SBSR), Sharda University, Greater Noida, 201310, India.

⁷Department of Chemistry, University of Petroleum & Energy Studies, Energy Acres, Dehradun, 248007, India.

⁸Department of Chemical Pathology, School of Pathology, Faculty of Health Sciences and National Health Laboratory Service, University of the Free State, Bloemfontein, South Africa.

⁹Department of Life Sciences, School of Pharmacy, International Medical University, Bukit Jalil, Kuala Lumpur, 57000, Malaysia

¹⁰Discipline of Pharmacy, Graduate School of Health, University of Technology Sydney, Ultimo NSW, 2007, Australia.

[#]These authors have contributed equally to this work and share first authorship.

✉ Corresponding author. E-mail: harishdureja@gmail.com; harishdureja@mdu.ac.in; Tel.: +91-9416357995

Received: Sep. 17, 2021; **Accepted:** Mar. 20, 2022; **Published:** Apr. 22, 2022

Citation: Mandeep Dahiya, Rajendra Awasthi, Gaurav Gupta, Sachin Kumar Singh, Monica Gulati, Niraj Kumar Jha, Saurabh Kumar Jha, Ankur Sharma, Parteek Prasher, Krishnan Anand, Dinesh Kumar Chellappan, Kamal Dua, and Harish Dureja, Optimization Studies on Imatinib Mesylate Loaded Nanoliposomes Using Box-Behnken Design. *Nano Biomed. Eng.*, 2022, 14(1): 23-37.

DOI: 10.5101/nbe.v14i1.p23-37.

Abstract

Nanoliposomes are bilayer phospholipid vesicles used to encapsulate and deliver therapeutic agents. The study was aimed to investigate the effects of critical variables on nanoliposomes characteristics. Imatinib mesylate-loaded nanoliposomes were formulated by the two-step emulsification process using a high-speed homogenizer system and probe-type ultrasonicator. The Box-Behnken design was utilized to optimize the process parameters. The mean particle size of nanoliposomes was found to be 211 nm to 623.3 nm with a low value of polydispersity index (0.005 to 0.7). Zeta potential values varied from -27.6 mV to -9.2 mV in uncoated nanoliposomes to +27.5 mV in chitosan-coated nanoliposomes. The encapsulation efficiency in formulation NLP-H8 containing 200 mg of phosphatidylcholine, homogenization speed of 12000 rpm, and 7 min of sonication time was found to be 76.49% without the coating and 85.4% in 0.2% w/v chitosan-coated nanoliposomes. TEM image confirmed the spherical shape of nanoliposomes. *In-vitro* drug release study demonstrated that the optimized nanoliposomal formulations released 84.67% of the loaded drug after 24 h in 0.1 N HCl. The IC₅₀ value of formulation NLP-H8 was found to be 7.98 μM. Nanoliposomal formulations were prepared successfully with suitable size, morphology, encapsulation efficiency, and drug release. The models developed in this study may be utilized further as a response surface for the various parameters of nanoliposomes.

Keywords: Imatinib mesylate, Nanoliposome, Emulsification, Box-Behnken design, Ultrasonication, cytotoxicity

Introduction

Nanoliposomes consisting of phosphatidylcholine

and cholesterol are biocompatible, biodegradable, and nontoxic drug carriers [1]. These vesicular delivery systems have been utilized for achieving many

objectives like targeting of drugs bioavailability as well as increasing their stability [2]. Nanoliposomes have shown promising applications in pharmaceutical research due to their improved absorption and targeting effect [3, 4]. Nanoliposomes loaded with active agents can target the tumor cells actively or passively. Passive targeting allows nanoliposomes to accumulate in the tumor by enhanced permeability and retention effect [5]. Nanoliposomes can simultaneously incorporate and release two drugs with different solubility. The lipids used in the synthesis of nanoliposomes are reported for liver protection, memory enhancement, and reduced cholesterol absorption from the intestine. These intriguing advantages of nanoliposomes make them superior over the other reported nanoformulations [6]. Surface modification of liposomes has been reported to stabilize liposomal vesicles in different environmental conditions and to avoid rapid leakage of encapsulated drugs [7]. Chitosan, a biocompatible polymer, has been reported to improve the efficiency of conventional liposomal vesicles in terms of stability of drug release and for target-specific drug delivery [8-11]. Chitosan can improve drug penetration and absorption across the mucosal epithelia due to its mucoadhesive property [8].

The phospholipids make a bilayered concentric sphere with bilayer membranes and a central compartment [12]. The nanoliposomes permit the active agents having diverse physicochemical properties to be encapsulated into the internal compartment and the bilayers. The nanoliposomes solubilize hydrophobic drugs, improve their stability, alter blood circulation properties of active agents, and consequently increases their aggregation into tumor tissues [13]. Despite the ongoing investigations on nanoliposome-based chemotherapy delivery systems, the formulation methods need to be optimized for dependable and reproducible production, and physicochemical attributes should be clarified for the expansion of more advanced systems [14]. Box-Behnken design is a family of three-level designs that are efficient in fitting second-order response surfaces and is based on the construction of balanced incomplete block designs [15]. In this study, a nanoliposomal delivery system of imatinib mesylate was prepared and the characteristics of the system were studied.

Nanoliposomes prepared by the emulsification method have high encapsulation of both the hydrophilic and lipophilic drugs. Emulsification method

replaces water-immiscible solvent with an aqueous phase [16]. The rationale to select a most promising two-step emulsification approach in the synthesis of nanoliposomes is the cumulation of advantage of sonication energy to obtain thermodynamically stable bilayer vesicles. Sonication is commonly used as an energy source for the lipid molecule organization during the formation of bilayer vesicles. Sonication is also often employed to reduce the number of bilayers and consequently the vesicle size. However, limited information on the exact mechanism of the effects of ultrasound on nanoliposomal vesicle formation is available [6].

Imatinib mesylate, a selective tyrosine kinase receptor inhibitor, is an oral chemotherapy medication used to treat cancer. Pharmacokinetic studies showed an absolute oral bioavailability of imatinib mesylate is 98% from various oral dosage forms like a solution, capsule, and tablet. The elimination half-life of imatinib mesylate is about 18 h. Imatinib mesylate primarily binds to albumin and α 1-acid glycoprotein (95%) [17]. Imatinib mesylate is the standard treatment option for gastrointestinal stromal tumors and chronic myeloid leukemia. However, it has minimal therapeutic activity as a second-line treatment of metastatic cervical cancer expressing platelet-derived growth factor receptor, and solid tumors like ovarian and prostate cancer. The treatment failure could be due to the low drug concentration at the target site [18].

The purpose of this study is to investigate the effects of critical formulation variables on nanoliposomes characteristics and to explore the potential of synthesized nanoliposomal formulation for controlled delivery of imatinib mesylate. To achieve this objective, imatinib mesylate-loaded nanoliposomes were formulated by the two-step emulsification process using a high-speed homogenizer system and probe-type ultrasonicator. The Box-Behnken design was utilized to optimize the process parameters. The effect of independent variables like phosphatidylcholine concentration (% w/v), homogenizer speed (rpm), and sonication time (min) was examined on entrapment efficiency, loading capacity, zeta potential, and cumulative drug release. The synthesized nanoliposomes were subsequently characterized for size, zeta potential, polydispersity index, entrapment and loading capacity, morphology, and *in vitro* drug release. Cytotoxicity study was carried out on A549 lung cancer cell lines.

Experimental

Materials

Imatinib mesylate was provided as a gift sample by Mac-Chem Products India Pvt. Ltd., Mumbai, India. Cholesterol and phosphatidylcholine were obtained from Central Drug House (P) Ltd., New Delhi, India. HPLC grade acetonitrile and ammonium acetate were obtained from Fisher Scientific, Mumbai, India, and Rankem, New Delhi, India, respectively. Diethyl ether and Tween 80 were obtained from Loba Chemie, Mumbai, India. Dialysis tubing membrane was procured from HiMedia Laboratories, Mumbai, India. All other chemicals were of analytical grade and used as received without further processing.

Methods

Preparation of imatinib mesylate loaded nanoliposomes

Nanoliposomes were formulated using a two-step emulsification approach [19]. Briefly; phosphatidylcholine (125-200 mg) and cholesterol (45 mg) were dissolved in cyclohexane. Imatinib mesylate (100 mg) was dissolved in distilled water (W1). The

lipid phase (20 mL) and the aqueous phase (10 mL) were taken in a 50 mL beaker and the emulsification was carried out using IKA T-25 ULTRA-TURRAX digital high-speed homogenizer at 8000-16000 rpm for 1 min to form W1/O type emulsion (primary emulsion). The primary emulsion was sonicated using a probe-type sonicator (Sonics Vibra Cell, USA) for 3-7 min (10 sec ON and 10 sec OFF cycles) to avoid phase separation. The temperature was maintained at 25 °C. The primary nanoemulsion was mixed with an aqueous phase (W2) containing phosphate buffer (pH 7.4, 10 mL) and Tween 80. Emulsification was carried at 18000 rpm for a period of 30 sec to produce nanoliposomes.

Optimization of nanoliposomes using Box-Behnken design

Box-Behnken design (Version 11.0.4.0, Design Expert[®] Software, Stat-Ease Inc., Minneapolis, MN) was used to study the effect of phosphatidylcholine concentration (X_1), homogenizer speed (X_2), and sonication time (X_3) on encapsulation efficiency, loading capacity, zeta potential and in-vitro drug release (Table 1).

Table 1 Box-Behnken design with the levels of independent variables to formulate imatinib mesylate-loaded nanoliposomes

Formulation code	Concentration of phosphatidylcholine (% w/v) (X_1)	Homogenizer speed (rpm) (X_2)	Sonication time (min) (X_3)
NLP-H1	-1(125)	-1(8000)	0(5)
NLP-H2	+1(200)	-1(8000)	0(5)
NLP-H3	-1(125)	+1(16000)	0(5)
NLP-H4	+1(200)	+1(16000)	0(5)
NLP-H5	-1 (125)	0(12000)	-1(3)
NLP-H6	+1(200)	0(12000)	-1(3)
NLP-H7	-1(125)	0(12000)	+1(7)
NLP-H8	+1(200)	0(12000)	+1(7)
NLP-H9	0(162.5)	-1(8000)	-1(3)
NLP-H10	0(162.5)	+1(16000)	-1(3)
NLP-H11	0(162.5)	-1(8000)	+1(7)
NLP-H12	0(162.5)	+1(16000)	+1(7)
NLP-H13	0(162.5)	0(12000)	0(5)
NLP-H14	0(162.5)	0(12000)	0(5)
NLP-H15	0(162.5)	0(12000)	0(5)
NLP-H16	0(162.5)	0(12000)	0(5)
NLP-H17	0(162.5)	0(12000)	0(5)

Levels for independent variables			
Codes for different levels of independent variables	Concentration of phosphatidylcholine (% w/v) (X_1)	Homogenizer speed (rpm) (X_2)	Sonication time (min) (X_3)
Low (-1)	125	8000	3
Medium (0)	162.5	12000	5
High (+1)	200	16000	7

*Values in bracket indicate the real values.

Characterization of nanoliposomes

Particle size, zeta potential, and polydispersity index

Nanoliposomes (1 mL) were dispersed in phosphate buffer solution (pH 7.4, 10 mL) to estimate particle size. The samples were filled in a polystyrene corvette in the hydro dispersing unit and 64 runs per sample scan were taken. The average diameter of all the runs was recorded as cumulant diameter. Particle size analysis, polydispersity index (PDI), and zeta potential analysis were carried using Zetasizer (Nano-ZS90, Malvern Instruments, Malvern, UK). PDI was determined as a measure of particle size distribution using the dynamic light scattering approach [20, 21].

Determination of encapsulation efficiency and loading capacity

Encapsulation efficiency and loading capacity were determined by lysis of imatinib mesylate-loaded nanoliposomes in methanol [22]. The mixture was sonicated for 3 min. The concentration of imatinib mesylate was assayed using the high-performance liquid chromatography (HPLC) method (1200 series, Agilent Technologies, Germany). The system consisted of a stainless-steel column (25 cm × 4.6 mm) packed with octadecylsilane bonded to porous silica (3 μm). A mixture of acetonitrile and 1% w/v ammonium acetate (60:40) were used as mobile phase at a flow rate of 0.7 mL/min. The sample analysis was carried out at 254 nm. Each sample was analyzed in triplicate.

Thermal analysis

Thermal analysis of imatinib mesylate, cholesterol, phosphatidylcholine, physical mixture, and the optimized formulation was carried to find out the compatibility between components and crystalline behavior using differential scanning calorimeter (DSC Q10 V9.9, Waters Corporation, USA). Indium was used as standard material to calibrate the instrument. The samples were analyzed in a sealed aluminum pan (heating range 30-300 °C, 10 °C/min) under a nitrogen atmosphere (60 mL/min). An empty aluminum pan was used as a reference [23].

Fourier transform infrared (FTIR) spectroscopy

FTIR spectrums of imatinib mesylate, physical mixture, and optimized formulation (formulation NLP-H8) were recorded using a FTIR spectrophotometer (FTIR Alpha Bruker 1206 0280, Germany). Samples were finely grounded and mixed with potassium bromide. The mixture was pressed

into pellets using a KBr press. The spectrums were recorded over the range of 4000-400 cm⁻¹. The drug was identified by characteristic peaks obtained and compared with the literature [24].

Morphological characterization

Morphology and surface-appearance of nanoliposomes were examined *via a* high-resolution transmission electron microscope (HRTEM, FEI Company Tecnai TF20, Hillsboro, Oregon, USA). The TEM facility consisted of a 200 KV TEM equipped with a high brightness field-emission gun source which enhanced resolution and sensitivity. TEM was equipped with a 4 K × 4 K Eagle CCD (charged coupled device) camera with a 4-port readout. Samples (5 μL) were placed onto the carbon film-coated copper grid (300 mesh size) and allowed for 2 min to settle down. The sample-loaded grid was stained with 5 μL of 2% uranyl acetate (negative stain) and allowed to settle down for 2 min. The excess amount of stain was removed using tissue paper. The grid was dried for 3 h and examined [25].

Cytotoxicity study

Cell culture and treatment

For the cytotoxicity study, A549 lung cancer cell lines were procured from National Centre for Cell Science, Pune, India, and developed in DMEM (Dulbecco's Modified Eagle's Medium) consisting of 10% FBS (fetal bovine serum), 100 units/mL penicillin, and 100 μg/mL streptomycin. The cells were maintained at 37 °C in a 5% carbon dioxide humidified incubator. Once the cell became confluent, the culture medium was removed and washed with 1% phosphate buffer saline (PBS, pH 7.2) solution to inactivate the existing medium in the culture. Trypsin-EDTA 0.25% (w/v) solution treatment was carried out for the trypsinization. Consequently, trypsin was inactivated by adding DMEM media. Centrifugation was carried out at 1200 rpm and 37 °C for 5 min to collect the cells. The maintenance of the cultured cell line was done in a 25 cm² flask. The same steps were repeated for maintaining the cells [26, 27].

MTT assay

The anti-proliferative potential of formulation NLP-H8 and NLP-H12 was estimated using 3-(4,5-dimethylthiazol-2-yl)-2,5-diphenyl tetrazolium bromide (MTT) assay method. The assay was carried out in a 96-well plate. The medium (100 μL) was filled in each well; the treatment received two concentrations

viz., 1, and 5 μM and incubated for 24 h. After 24 h, the medium was discarded and washed with $1\times$ PBS (pH 7.2) and treated with MTT dye (5 mg in 10 mL of $1\times$ PBS). The sample was incubated at room temperature in the dark for 4h to form formazan crystals. The crystals were dissolved in dimethyl sulfoxide and the absorbance was recorded spectrometrically using a microplate reader at 570 nm. The result was established by comparing the data in triplicate [28].

In-vitro drug release study

In-vitro release of imatinib mesylate from the nanoliposomes was assessed using the dialysis bag diffusion method. Dissolution study was carried out using acidic (0.1 N HCl, pH 1.2) and alkaline (phosphate buffer pH 7.4) conditions. The acidic and alkaline media were selected to simulate the gastric and intestinal pH, respectively. For the activation of the dialysis membrane, glycerol was removed by washing with running water for 3 h. The tubing was treated with a 0.3% w/v solution of sodium sulfide at 80 °C for 1 min to remove sulfur compounds. Washing by hot water (60 °C) was carried out for 2 min, followed by treatment with 0.2% v/v sulfuric acid. Further, the tubing was rinsed with hot water to remove any traces of the acid. Further, the tubing was washed three times with double distilled water [29].

The nanoliposomes (2 mL) were transferred in a cellulose dialysis bag (molecular weight cut-off 12000 Da; HiMedia, Mumbai, India) and sealed at both ends. The dialysis bag was plunged in the cylindrical vessel of USP dissolution apparatus II (DS 8000, Lab India, Mumbai, India) containing 200 mL of dissolution medium maintained at 37 ± 0.5 °C. The paddle was rotated at 75 rpm. The aliquots (2 mL) were withdrawn at predetermined time intervals (0.5, 1, 2, 4, 6, 8, 12, 18, and 24 h) and replaced with an equal volume of fresh medium. The samples were analyzed by the HPLC system (Agilent Technologies, 1200, Germany) using a quaternary pump, Eclipse XDB-C18 column (4.6 mm \times 150 mm). The mobile phase contained a mixture of 1% ammonium acetate and acetonitrile (40:60). The solvent flow rate was maintained at 0.7 mL/min and the samples were analyzed at 254 nm. The sampling was carried out in triplicate [30].

Drug release kinetics study

To determine the *in-vitro* release kinetics of imatinib mesylate, the release data were fitted to zero-order and first-order equations. Further, to determine the exact release mechanism, the dissolution data were plotted

according to Higuchi's and Korsmeyer-Peppas' models [31].

Stability studies

The stability study of optimized nanoliposome formulation (formulation NLP-H8) stored at freeze temperature (4 ± 1 °C), room temperature (25 ± 2 °C/60% \pm 5% RH), and (45 ± 2 °C/75 \pm 5% RH) was carried out as per the ICH guidelines [32]. The formulation stability was evaluated in terms of particle size and *in-vitro* release profile for a period of 3 months.

Coating with biopolymer

Optimized formulation (formulation NLP-H8) was coated with chitosan. Chitosan solutions (0.1% w/v and 0.2% w/v) were prepared in double-distilled water containing 0.1% v/v glacial acetic acid at 40 °C. The solutions were filtered using a microfiltration system (Pioneer Scientific Instrument Corporation, Kolkata, India) for the removal of impurities, if any. The chitosan solution was added dropwise in an equivalent volume of imatinib mesylate-loaded nanoliposomal formulation and mixed for 3 h using a magnetic stirrer at 25 °C. To allow the formation of a chitosan layer, the mixture was incubated overnight at 4 °C. The effect of coating was evaluated in terms of particle size, zeta potential, encapsulation efficiency, and loading capacity [33, 34].

Comparison with marketed formulation

The *in-vitro* drug release profile of imatinib mesylate from the optimized chitosan-coated nanoliposomal formulation (formulation NLP-H8) was compared with the marketed formulation of imatinib mesylate (Imalek, Sun Pharmaceuticals Industries Ltd., Mumbai, India) by the method described in section 3.7.

Statistical analysis

To study the level of significance, the encapsulation efficiency, loading capacity, zeta potential, drug release data were statistically analyzed by two-way analysis of variance (ANOVA) using Design Expert Software (Version 11.0.4.0, Stat-Ease Inc., Minneapolis, MN). F-test was used to compare regression mean square with a residual mean square. The p-value of <0.05 was considered statistically significant.

Results and Discussion

Mathematical and statistical design

The quadratic models were generated to establish

the significance of the study. The real values of factors were transformed to facilitate orthogonality of results and easy calculation. The effect plots are shown in Fig. 1. Three-dimensional response surface plots and the corresponding contour plots for the responses are shown in Fig. 2 and Fig. 3. Mathematical models were developed for the estimation of parameters as below:

$$Y_1 = 57.20 + 4.38X_1 + 5.87X_2 + 1.61X_3 + 0.53X_1X_2 + 2.72X_1X_3 - 0.532X_2X_3 + 5.81X_1^2 - 2.80X_2^2 + 3.24X_3^2,$$

$$Y_2 = 39.96 + 4.99X_1 + 5.26X_2 + 1.31X_3 + 0.307X_1X_2 + 1.27X_1X_3 - 0.7X_2X_3 + 7.62X_1^2 - 4.07X_2^2 + 3.93X_3^2,$$

$$Y_3 = -25.26 - 0.0875X_1 - 3.04X_2 - 1.85X_3 + 4.9X_1X_2 + 1.43X_1X_3 + 4.07X_2X_3 + 3.53X_1^2 + 4.53X_2^2 + 0.405X_3^2,$$

$$Y_4 = 75.48 + 1.81X_1 + 5.54X_2 + 0.905X_3 + 0.435X_1X_2 + 0.3525X_1X_3 + 2.75X_2X_3 + 1.55X_1^2 + 0.0815X_2^2 + 4.85X_3^2,$$

$$Y_5 = 42.06 + 3.75X_1 + 7.52X_2 + 0.9237X_3 + 1.36X_1X_2 + 0.0175X_1X_3 + 2.84X_2X_3 - 0.0105X_1^2 - 2.24X_2^2 + 7.25X_3^2,$$

where Y_1 = encapsulation efficiency, Y_2 = loading capacity, Y_3 = zeta potential, Y_4 = percentage cumulative drug release in 0.1N HCl (pH 1.2), Y_5 = percentage cumulative drug release in phosphate buffer (pH 7.4), X_1 = concentration of phosphatidyl choline (% w/v), X_2 = homogenizer speed (rpm), and X_3 = sonication time (min), X_1X_2 , X_1X_3 , X_2X_3 are interaction term, and X_1^2 , X_2^2 and X_3^2 are quadratic relationship terms.

Particle size, zeta potential, and polydispersity index

Particle size, PDI, and zeta potential values ranged

from 211 nm to 623.3 nm, 0.005 to 0.700, and -27.6 mV to -9.2 mV, respectively (Table 2). The formulation containing 200 mg of phosphatidylcholine, homogenizer speed of 16000 rpm with 5 min of sonication time (formulation NLP-H4) had the smallest particle size (211 nm) and PDI value of 0.173. The formulation containing 162.5 mg of phosphatidylcholine, homogenizer speed 12000 rpm with 5 min of sonication time (formulation NLP-H14) had a zeta potential value of -27.6 mV. The smallest particle size was obtained at a higher concentration of phosphatidylcholine, high homogenization speed, and mid-value of sonication time. The highest zeta potential value was obtained at the mid-value of all three factors.

Encapsulation efficiency and loading capacity

The results of percentage drug encapsulation are presented in Table 2. The formulation containing 200 mg of phosphatidylcholine, homogenization speed of 12000 rpm, and 7 min sonication (formulation NLP-H8) had the highest loading capacity (62.36%) and highest encapsulation efficiency (76.49%) (Table 2). High encapsulation efficiency and loading capacity were obtained at a higher concentration of phosphatidylcholine, mid-value of homogenization speed, and high sonication time.

Thermal analysis

The nano-encapsulation process offers a considerable reduction in the crystallinity of the

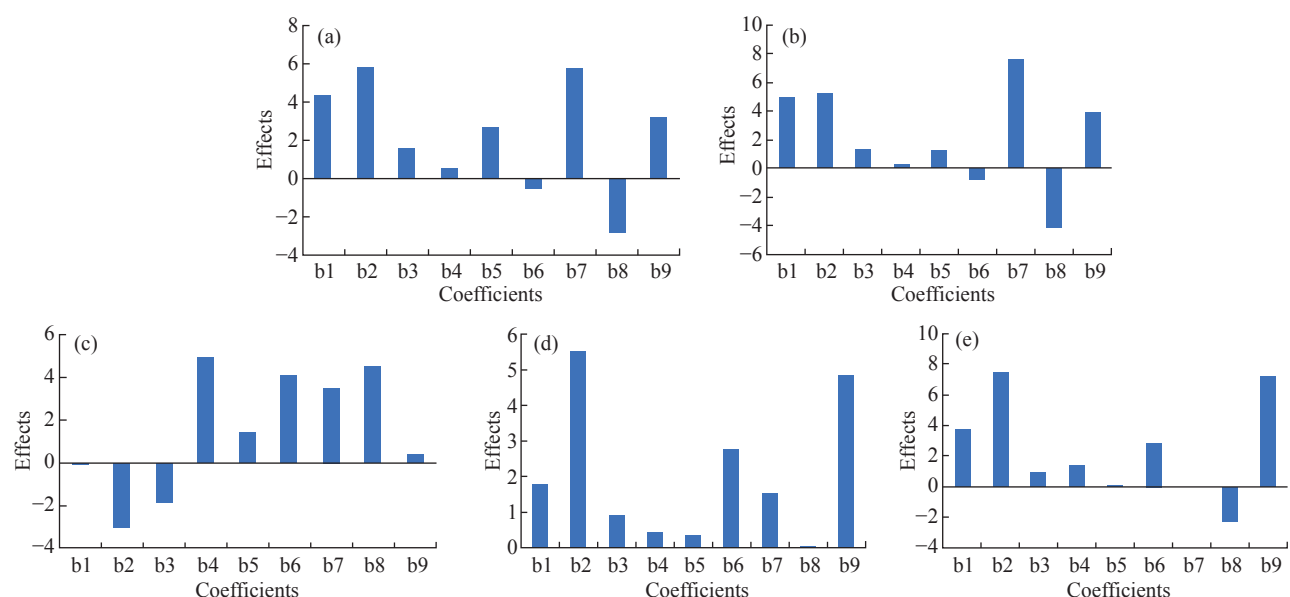


Fig. 1 Effect plots of coefficients of parameters: (a) Encapsulation efficiency, (b) Loading capacity, (c) Zeta potential, (d) Cumulative drug release in 0.1 N HCl, and (e) Cumulative drug release in phosphate buffer pH 7.4 (b1, b2, b3 = coefficients of main effects; b4, b5, b6 = coefficient of interaction terms and b7, b8, b9 = coefficients of square terms).

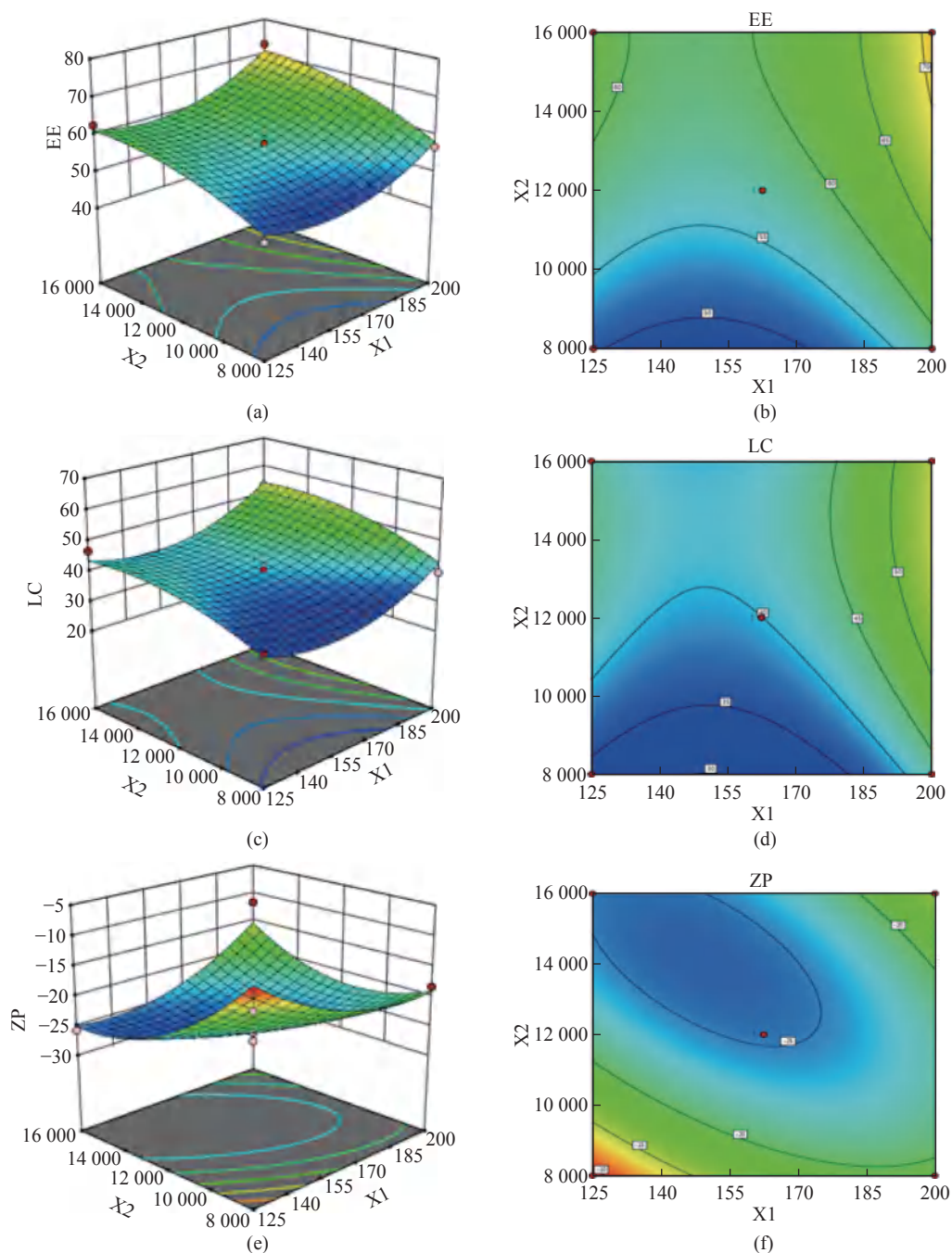


Fig. 2 3D Response surface and contour plot of parameters as a function of formulation variables: **(a) & (b)** Encapsulation efficiency; **(c) & (d)** Loading capacity and **(e) & (f)** Zeta potential, X1: phosphatidylcholine (mg), X2: homogenizer speed (rpm).

drug and allows a nearly amorphous state [35]. The DSC thermogram of imatinib mesylate showed an endothermic peak at 229.54 °C corresponding to its melting point (230.35°C) with a percentage purity of 96.24% (Fig. 4(a)). The DSC thermogram of the optimized batch (formulation NLP-H8) is shown in Fig. 4(b). DSC thermogram of cholesterol (Fig. 4(c)) and phosphatidylcholine (Fig. 4(d)) showed sharp endothermic peaks at 151.12 °C and 140.01 °C, respectively. The thermogram of the physical mixture displayed compatibility between the drug and

other formulation components. The dissipation of the endothermic peak of the drug in the optimized batch (formulation NLP-H8) indicated a molecular dispersion of the drug inside the nanoliposomal system.

Fourier transform infrared spectroscopy

FTIR spectra were used to study the interaction between imatinib mesylate, cholesterol, and phosphatidylcholine, if any. FTIR spectrum of pure imatinib mesylate showed a characteristic peak at 3258.35 cm^{-1} corresponding to N-H stretching.

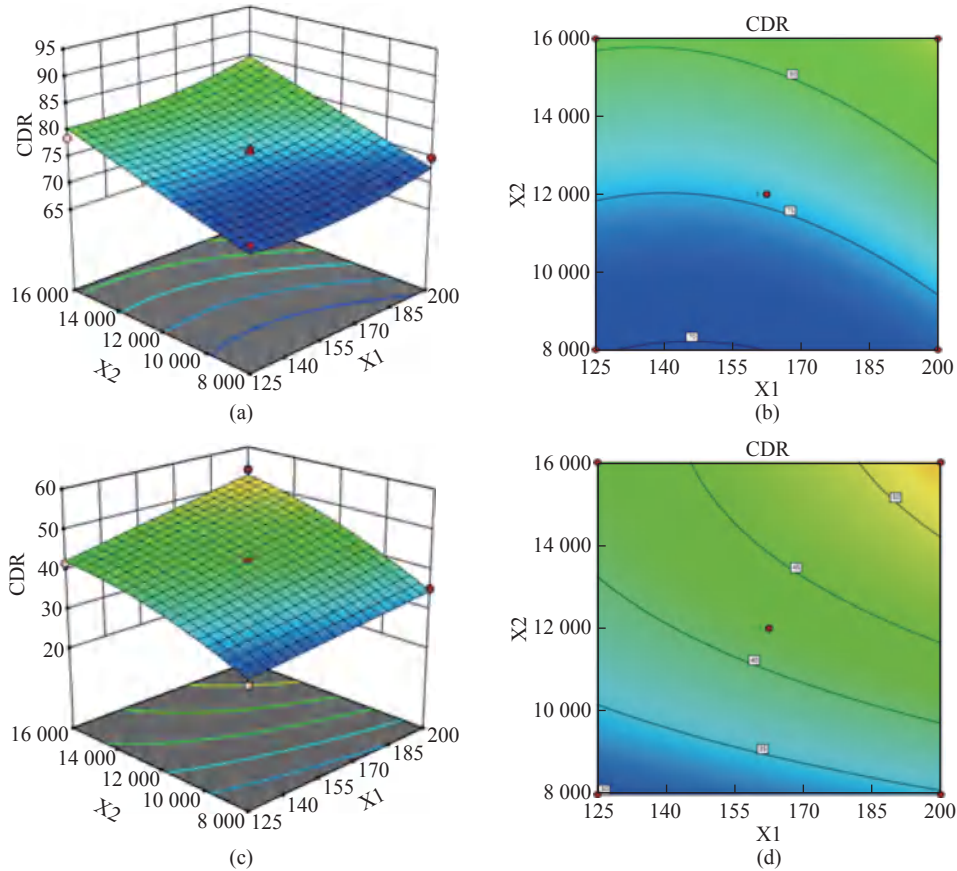


Fig. 3 3D Response surface and contour plots of cumulative drug release (CDR%) as a function of formulation variables: **(a) & (b)** 0.1 N HCl and **(c) & (d)** Phosphate buffer pH 7.4. X1: phosphatidylcholine (mg), X2: homogenizer speed (rpm).

Table 2 Results of *in-vitro* characterization of imatinib mesylate-loaded nanoliposomes

Formulation code	Particle size (nm)	Polydispersity index	Zeta potential (mV)	Encapsulation efficiency (%)	Loading capacity (%)
NLP-H1	618.5	0.379	-12.9	48.67±0.34	34.42±0.23
NLP-H2	420.7	0.097	-18.4	56.79±0.71	39.68±0.31
NLP-H3	231.2	0.188	-25.8	62.56±0.46	46.74±0.39
NLP-H4	211	0.173	-11.7	72.80±0.39	53.23±0.51
NLP-H5	368.6	0.167	-16.4	61.44±0.55	43.21±0.28
NLP-H6	267.6	0.178	-23.9	64.34±0.37	54.77±0.37
NLP-H7	358.1	0.217	-21.6	62.7±0.44	45.73±0.24
NLP-H8	286.6	0.211	-23.4	76.49±0.89	62.36±0.43
NLP-H9	623.3	0.700	-9.2	52.97±0.46	34.97±0.55
NLP-H10	220.9	0.240	-26.4	62.56±0.38	44.49±0.43
NLP-H11	389.2	0.062	-22.4	53.77±0.71	36.56±0.27
NLP-H12	217.9	0.005	-23.3	61.23±0.55	43.28±0.18
NLP-H13	225.2	0.194	-26.2	57.82±0.41	40.39±0.63
NLP-H14	216.5	0.139	-27.6	56.93±0.26	39.67±0.59
NLP-H15	248.8	0.197	-24.2	57.23±0.32	40.55±0.35
NLP-H16	254.7	0.025	-23.7	57.59±0.48	39.89±0.27
NLP-H17	251.6	0.177	-24.6	56.43±0.22	39.32±0.43

The peak at 2941.13 cm^{-1} corresponds to $=\text{CH}_2$ stretching. The peaks around 1657.02 cm^{-1} and 1437.22 cm^{-1} corresponding to $\text{C}=\text{O}$ stretching and $\text{C}-\text{H}$ deformation, respectively. The peak at 1305.31 cm^{-1} corresponds to $\text{C}=\text{N}$ stretching (Fig. 5(a)).

FTIR spectrum of the physical mixture showed a characteristic peak at 3261.59 cm^{-1} corresponding to $\text{N}-\text{H}$ stretching. The peak at 2929.11 cm^{-1} corresponds to $=\text{CH}_2$ stretching. The peaks around 1657.93 cm^{-1} and 1451.03 cm^{-1} corresponding to $\text{C}=\text{O}$ stretching

and C–H deformation, respectively. The peak at 1321.02 cm⁻¹ corresponds to C=N stretching (Fig. 5(b)). FTIR spectrum of formulation NLP-H8 showed a characteristic peak at 3254.08 cm⁻¹ corresponding to N-H stretching. The peak at 2931.36 cm⁻¹ corresponds

to =CH₂ stretching. The peaks around 1641.90 cm⁻¹ and 1461.69 cm⁻¹ corresponding to C=O stretching and C-H deformation, respectively (Fig. 5(c)). No significant shifting in peak position, no overlapping of characteristic peaks, and no appearance of new peaks

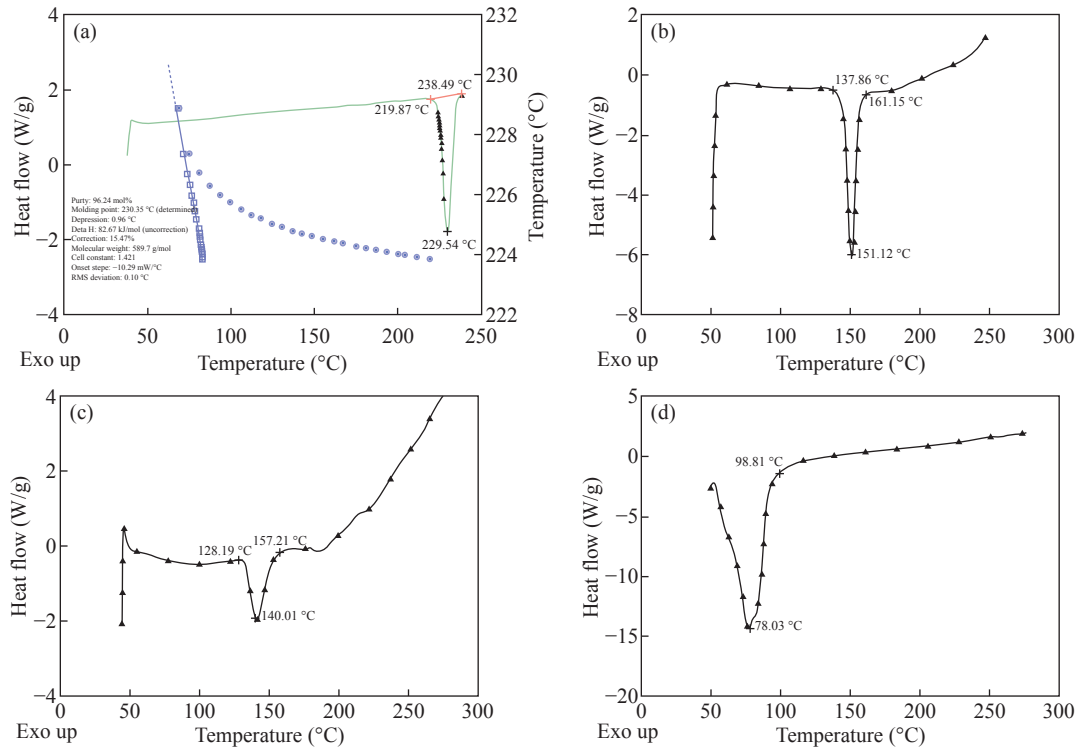


Fig. 4 DSC thermogram of (a) Imatinib mesylate, (b) Cholesterol, (c) Phosphatidylcholine, and (d) Optimized batch (formulation NLP-H8).

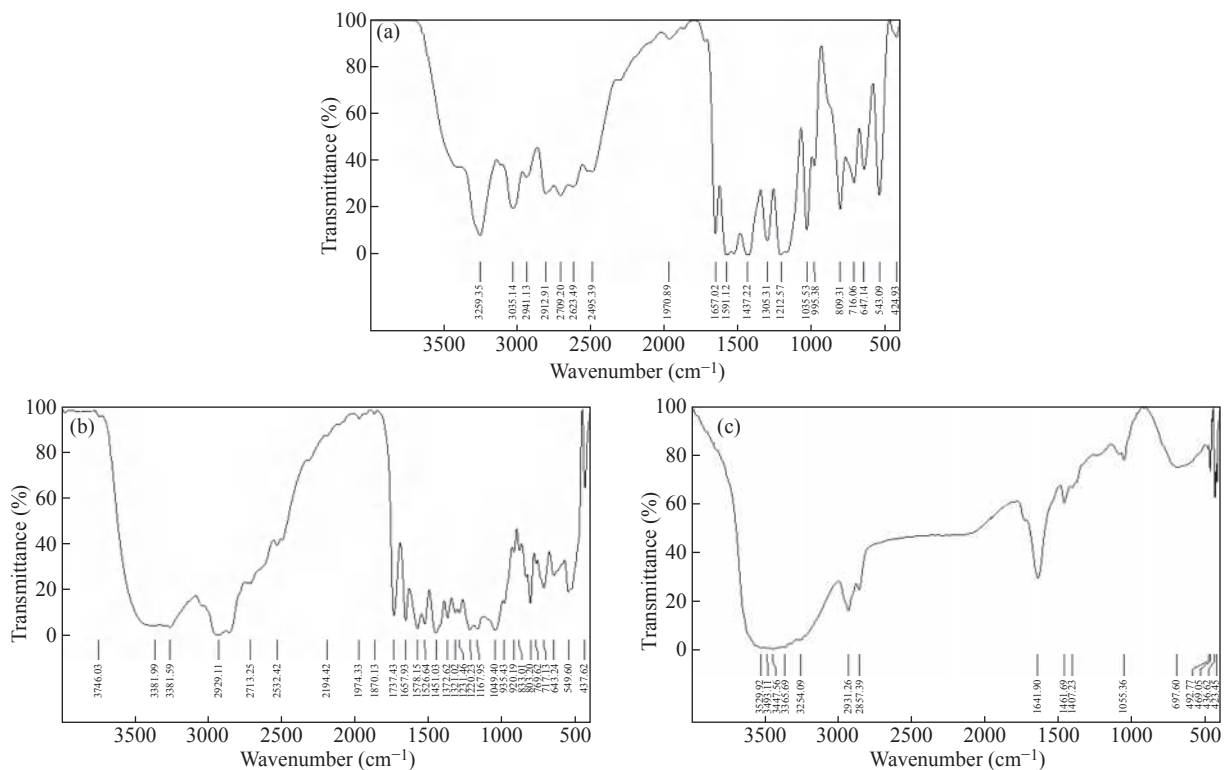


Fig. 5 FTIR spectrum of (a) Imatinib mesylate, (b) Physical mixture, and (c) Optimized batch (formulation NLP-H8).

was observed in optimized batch NLP-H8. The results indicated the stability of the drug and no molecular or chemical interaction between the drug and other components.

Morphological characterization

The TEM image of optimized imatinib mesylate loaded nanoliposomes (formulation NLP-H8) is shown in Fig. 6. The formulated imatinib mesylate-loaded nanoliposomes were found to be spherical in shape.

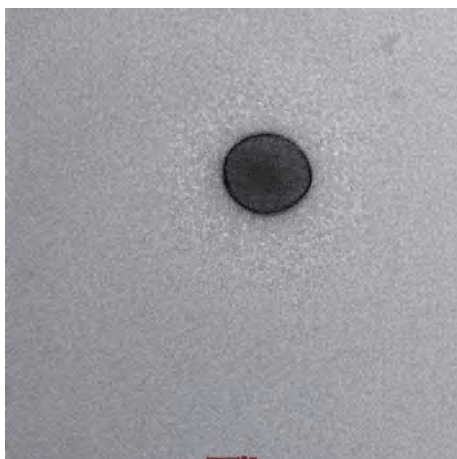


Fig. 6 Transmission electron microscopic image of optimized batch (formulation NLP-H8).

Cytotoxicity studies

Cytotoxic activity of pure imatinib mesylate and imatinib mesylate loaded nanoliposomes (formulation NLP-H8 and NLP-H12) was examined to compare the impact of highest drug encapsulation (formulation NLP-H8) and maximum drug release (formulation NLP-H12). Free imatinib mesylate had more cytotoxicity than the imatinib mesylate-loaded nanoliposomes (formulation NLP-H8 and NLP-H12). Less cytotoxicity of imatinib mesylate from nanoliposomes (formulation NLP-H8 and NLP-H12) might be due to its slow release. The IC_{50} value of free imatinib mesylate, formulation NLP-H8, and formulation NLP-H12 was 1.3, 7.98, and 13.22 μ M, respectively (Fig. 7). The results indicated that the cytotoxicity of imatinib mesylate could be associated with the particle size and zeta potential of synthesized nanoliposomes.

In-vitro release

The *in-vitro* drug release of imatinib mesylate from the formulated nanoliposomes was evaluated in 0.1N HCl (pH 1.2) and phosphate buffer (pH 7.4) to confirm the release of imatinib mesylate in the stomach (acidic environment) and simulated

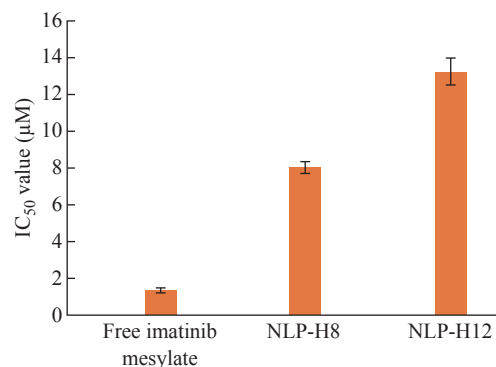


Fig. 7 Results of cytotoxic activity of pure imatinib mesylate and imatinib mesylate loaded nanoliposomes (formulation NLP-H8 and NLP-H12).

intestinal fluid (Fig. 8). Cumulative drug release in 0.1 N HCl ranged from 71.45% to 91.36% after 24 h dissolution study. Formulations containing 162.7 mg of phosphatidylcholine, homogenization speed 16000 rpm, and 7 min sonication time (formulations NLP-H12) had maximum imatinib mesylate release *i.e.*, 91.36% in 0.1 N HCl after 24 h. After 24h, cumulative drug release in phosphate buffer (pH 7.4) ranged from 28.45% to 58.47%. Formulation NLP-H12 had the maximum release of imatinib mesylate in phosphate buffer (pH 7.4) (58.47%) after 24 h. Imatinib mesylate is a free base and is more susceptible to dissolve in acidic media. This could be the reason for the sustained release of the imatinib mesylate profile in the 0.1N HCl and phosphate buffer (pH 7.4). However, the drug release was comparatively fast in 0.1N HCl. The sustained release of imatinib mesylate from the nanoliposomes may extend the drug absorption time in the gastrointestinal tract, which could enhance the therapeutic activity of the loaded drug and diminish its side effects.

Release kinetics

The *in-vitro* release data of formulation NLP-H12 was analyzed to determine the drug release kinetics using zero-order and first-order kinetic models. Further, the mechanism of imatinib mesylate release was accessed using Higuchi's and Korsmeyer-Peppas' equations. The regression linear *i.e.*, squared correlation coefficients (R^2) were determined from the mathematical models (Table 3). Higuchi's model had the highest R^2 value in the 0.1 N HCl, pH 1.2 (0.992) and in phosphate buffer, pH 7.4 (0.991). The 'n' values of the Korsmeyer-Peppas' model were 0.722 and 0.836, respectively in 0.1 N HCl and phosphate buffer (pH 7.4) indicating non-Fickian anomalous diffusion of imatinib mesylate from the synthesized nanoliposomes.

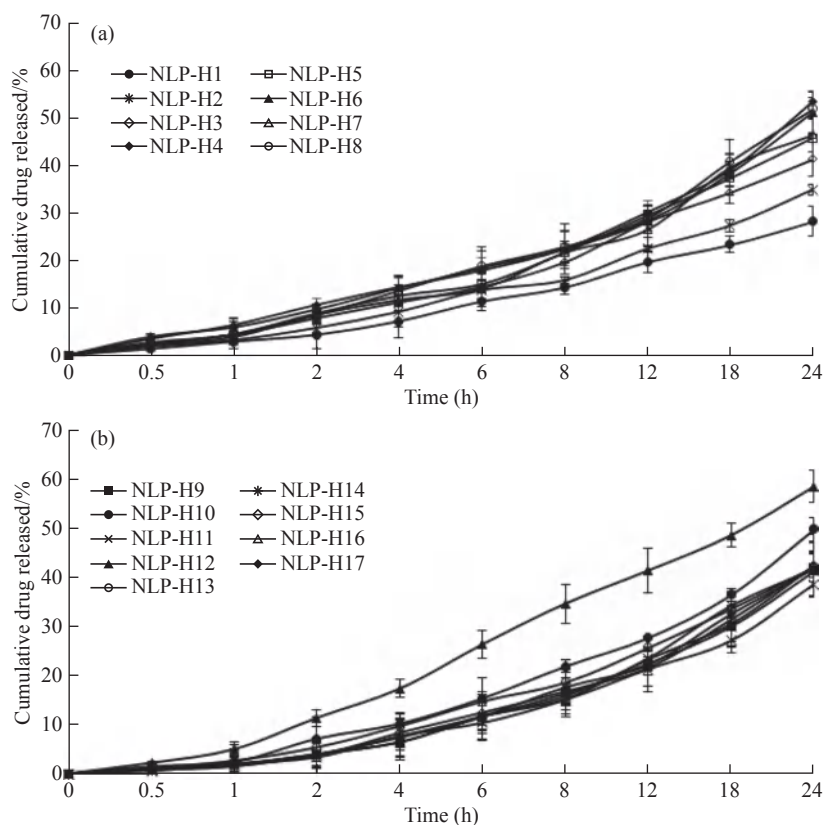


Fig. 8 *In-vitro* release profile of nanoliposomes in 200 mL of dissolution medium by cellulose dialysis bag method at 75 rpm (a) in 0.1 N HCl (filled circles : NLP-H1, cross lines: NLP-H2, empty diamonds: NLP-H3, filled diamonds: NLP-H4, empty squares: NLP-H5, filled triangles: NLP-H6, empty triangles: NLP-H7, empty circles: NLP-H8), and (b) in phosphate buffer pH 7.4 (filled squares: NLP-H9, filled circles: NLP-H10, cross lines: NLP-H11, filled triangles: NLP-H12, empty circles: NLP-H13, cross lines: NLP-H14, empty diamond: NLP-H15, empty triangle: NLP-H16, filled diamond: NLP-H17) at 37 °C (mean \pm SD, n = 3).

Table 3 Results of kinetic study for drug release from imatinib mesylate-loaded nanoliposomes

Kinetic model	Correlation coefficients (R^2)	
	0.1N HCl (pH 1.2)	Phosphate buffer (pH 7.4)
Zero-order	0.922	0.929
First-order	0.685	0.657
Higuchi's release model	0.992	0.991
Korsmeyer-Peppas' model	0.983	0.974
Value of n in Korsmeyer-Peppas' model	0.722	0.836

Stability studies

The optimized batch (formulation NLP-H8 stored at 4 ± 1 °C, 25 ± 2 °C/ $60 \pm 5\%$ RH and 45 ± 2 °C/ $75 \pm 5\%$ RH) was evaluated for particle size and percentage cumulative drug release after 30 days, 60 days, and 90 days. The formulation was found stable for a period of three months as no significant and considerable transformation was detected in the particle size and percentage cumulative drug release profile (Table 4). The increased size with time was due to the aggregation of particles. The increase in particle size was found to be least at 4 °C as compared with the formulation stored at 25 °C and 45 °C. The percentage

cumulative drug release decreased after storage. At 45 °C, the maximum fall in the percentage cumulative drug release was observed. Based on the results of stability studies the storage temperature of 4 °C is recommended for better storage stability.

Coating with biopolymer

The optimized batch (NLP-H8) was coated with chitosan. Particle size, encapsulation efficiency, and loading capacity increased after coating. Zeta potential increased significantly, indicating the stability of nanoliposomes (Table 5). The unpaired *t*-test was applied to correlate various parameters of uncoated nanoliposomes with 0.1% and 0.2 % w/v chitosan

Table 4 Effect of storage temperature on characteristics of imatinib mesylate-loaded nanoliposomes

Parameter	Temperature	Time intervals in months		
		1st	2nd	3rd
Particle size (nm)	4 °C	292.3	294.8	298.7
	Room temperature	295.4	301.5	304.2
	45 °C	297.9	305.2	307.4
Cumulative drug release (%) in 0.1N HCl (pH 1.2)	4 °C	83.33	81.67	78.46
	Room temperature	82.64	79.72	76.15
	45 °C	80.17	78.38	85.29
Cumulative drug release (%) in phosphate buffer (pH 7.4)	4 °C	54.11	52.47	50.68
	Room temperature	53.73	51.94	50.16
	45 °C	52.44	51.39	49.55

Table 5 Effect of coating with chitosan on particle size, zeta potential, encapsulation efficiency (%), and loading capacity (%)

Formulation code	Parameters							
	Particle size (nm)		Zeta potential (mV)		Encapsulation efficiency (%)		Loading capacity (%)	
Coating (% w/v)	0.1	0.2	0.1	0.2	0.1	0.2	0.1	0.2
NLP-H8	305.5	322.8	17.2	27.5	81.3±0.12	85.4±0.66	66.8±0.36	73.6±0.52

coating with regard to particle size and showed the statistically significant difference between coated and uncoated nanoliposomes (Table 6).

Comparison with marketed formulation

The *in-vitro* release profile of imatinib mesylate from optimized nanoliposomes (formulation NLP-H8) was compared to the marketed formulation (Imalek, Sun Pharmaceuticals Industries Ltd.) in 0.1 N HCl (pH 1.2) and phosphate buffer (pH 7.4) (Fig. 9).

Formulation NLP-H8 showed 8.86% and 4.35% of drug release in 0.1 N HCl (pH 1.2) and phosphate buffer (pH 7.4), respectively after 1 h. However, under similar dissolution conditions, the drug release from the marketed formulation was 78.27% and 37.83%, respectively. After 24 h, formulation NLP-H8 showed 84.67% and 52.41% of drug release in 0.1 N HCl (pH 1.2) and phosphate buffer pH 7.4 (pH 7.4), respectively; whereas the drug release from marketed formulation was 94.21% and 56.88% in 0.1 N HCl (pH

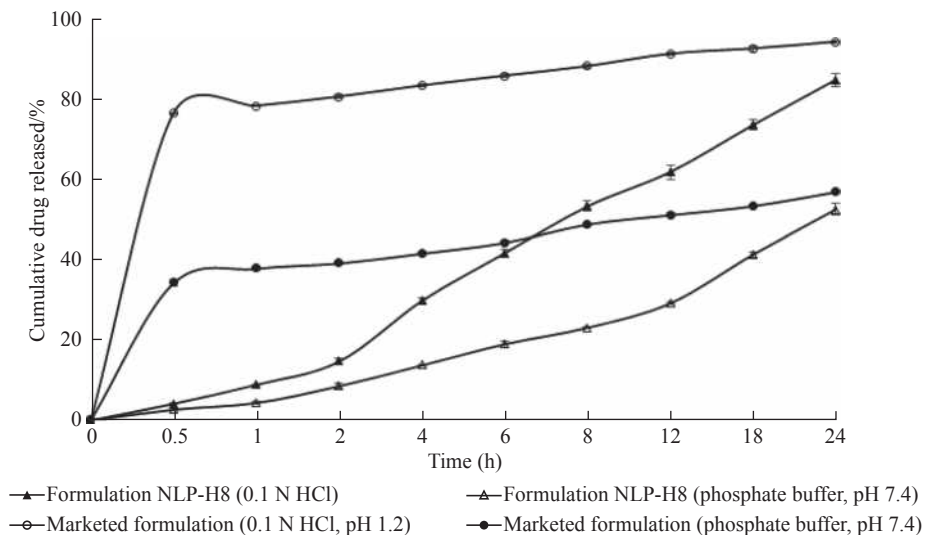


Fig. 9 Comparative *in-vitro* drug release profiles of optimized batch (formulation NLP-H8) and marketed formulation in 200 mL of dissolution medium by cellulose dialysis bag method at 75 rpm (filled triangles: optimized formulation NLP-H8 in 0.1 N HCl, pH 1.2, empty triangles: optimized NLP-H8 in phosphate buffer, pH 7.4, empty circles: marketed formulation in 0.1 N HCl pH 1.2, filled circles: marketed formulation in phosphate buffer, pH 7.4 at 37 °C (mean ± SD, n = 3).

Table 6 Unpaired t-test for NLP-H8 and coated NLP-H8 formulation with respect to particle size (P < 0.05; significant)

Parameter	Zeta potential		Encapsulation efficiency		Loading capacity	
	t value	P value	t value	P value	t value	P value
Chitosan coating (0.1% w/v)	13.3598	0.0056	22.2695	0.0020	23.8450	0.0018
Chitosan coating (0.2% w/v)	9.6910	0.0105	12.0039	0.0069	12.4902	0.0063

1.2) and phosphate buffer (pH 7.4), respectively. Slow drug release from nanoliposome may improve the therapeutic benefit of imatinib mesylate and reduce the side effects associated with conventional dosage forms.

Statistical analysis

On the application of two-way ANOVA, a significant difference was observed in the encapsulation efficiency, loading capacity, zeta potential, and drug release profiles among the formulations at a 95% confidence interval ($p < 0.05$), as the calculated F values were higher than the table values. There is only a 0.10% chance that a “model F-value” due to the noise (Table 7).

Conclusions

Imatinib mesylate-loaded nanoliposomes were prepared and optimized by a two-step emulsification process by utilizing Box-Behnken design. The developed nanoliposomes had a small particle size with a low value of polydispersity index. The encapsulation efficiency and loading capacity increased after coating with chitosan and zeta potential shifted towards the positive side. The developed mathematical models may be applied to formulate nanoliposomes with the required particle size, encapsulation efficiency, and drug release. *In-vitro* drug release study demonstrated sustained drug release from nanoliposomal

Table 7 Results of two-way ANOVA on the encapsulation efficiency, loading capacity, zeta potential, and release profiles of imatinib mesylate loaded nanoliposomes

Encapsulation efficiency					
	Degree of freedom	Sum of squares	Mean square	F	Significance (P < 0.05%)
Regression	9	699.09	77.68	11.7	0.0019
Residual	7	46.48	6.64	-	-
Total	16	745.57	-	-	-
Loading capacity					
Regression	9	817.23	90.80	10.91	0.0024
Residual	7	58.24	8.32	-	-
Total	16	875.47	-	-	-
Zeta potential					
Regression	9	421.28	46.81	4.57	0.0289
Residual	7	71.75	10.25	-	-
Total	16	502.41	-	-	-
Cumulative drug release in 0.1N HCl (pH 1.2)					
Regression	9	423.44	47.05	13.69	0.0012
Residual	7	24.06	3.44	-	-
Total	16	447.5	-	-	-
Cumulative drug release in phosphate buffer (pH 7.4)					
Regression	9	847.3	94.14	51.76	0.0001
Residual	7	12.73	1.82	-	-
Total	16	860.03	-	-	-

formulations. TEM analysis confirms the spherical shape of the optimized batch. The IC₅₀ value of formulation NLP-H8 was established to be 7.98 µM. Nanoliposomes could be utilized as prospective transporters for the delivery of imatinib mesylate. However, further research is needed to authenticate the bioavailability of imatinib mesylate nanoliposomes for oral applications.

Acknowledgements

This work was supported by the grant-in-aid to the Department of Pharmaceutical Sciences, Maharshi Dayanand University, Rohtak, India, under the plan of Major Research Project [F.No.-43-485/2014(SR)] by University Grants Commission, India.

Human and Animal Rights

No human or animal studies were carried out by the authors of this article.

Conflict of Interests

The authors declare that no competing interest exists.

References

- [1] B. Kapoor, R. Gupta, M. Gulati, et al., The why, where, who, how, and what of the vesicular delivery systems. *Adv Colloid Interface Sci*, 2019, 271: 101985.
- [2] B. Kapoor, R. Gupta, S.K. Singh, et al., Prodrugs, phospholipids and vesicular delivery - an effective triumvirate of pharmacosomes. *Adv Colloid Interface Sci*, 2018, 253: 35-65.
- [3] A. Akbarzadeh, R.R. Sadabady, S. Davaran, et al., Liposome: classification, preparation, and applications. *Nanoscale Res Lett*, 2013, 8(1): 102.
- [4] X. Luo, R. Guan, X. Chen, et al., Optimization on condition of epigallocatechin-3-gallate (EGCG) nanoliposomes by response surface methodology and cellular uptake studies in Caco-2 cells. *Nanoscale Res Lett*, 2014, 9(1): 291.
- [5] D. Rosenblum, N. Joshi, W. Tao, et al., Progress and challenges towards targeted delivery of cancer therapeutics. *Nat Commun* 2018, 9: 1410.
- [6] R. Koshani, S.M. Jafari, Ultrasound-assisted preparation of different nanocarriers loaded with food bioactive ingredients. *Adv Colloid Interface Sci*, 2019, 270: 123-146.
- [7] N. Oku, Y. Namba, Long-circulating liposomes. *Crit Rev Ther Drug Carr Syst*, 1994, 11: 231-270.
- [8] W. Zhou, C. Cheng, L. Ma, et al., The formation of chitosan-coated rhamnolipid liposomes containing curcumin: stability and *in vitro* digestion. *Molecules*, 2021, 26(3): 560.
- [9] S. Assadpour, J. Akhtari, M.R. Shiran, Pharmacokinetics study of chitosan-coated liposomes containing sumatriptan in the treatment of migraine. *Caspian J Intern Med*, 2022, 13(1): 90-99.
- [10] E. Yang, H.S. Jung, P.S. Chang, Stimuli-responsive polymer-complexed liposome nanocarrier provides controlled release of biomolecules. *Food Hydrocoll*, 2022, 125: 107397.
- [11] Hamedinasab H, Rezayan AH, Mellat M, et al. Development of chitosan-coated liposome for pulmonary delivery of N-acetylcysteine. *Int J Biol Macromol*, 2020, 156: 1455-1463.
- [12] V.P. Torchilin, Recent advances with liposomes as pharmaceutical carriers. *Nat Rev Drug Discov*, 2005, 4: 145-160.
- [13] A.S.A. Lila, T. Ishida, Liposomal delivery systems: design optimization and current applications. *Biol Pharm Bull*, 2017, 40: 1-10.
- [14] D. Pompeu, E. Silva, H. Rogez, Optimisation of the solvent extraction of phenolic antioxidants from fruits of *Euterpe oleracea* using response surface methodology. *Bioresource Technol*, 2009, 100: 6076-6082.
- [15] V. Mishra, S. Thakur, A. Patil, et al., Quality by design (QbD) approaches in current pharmaceutical set-up. *Expert Opin Drug Deliv*, 2018, 15(8): 737-758.
- [16] A. Wagner, K. Vorauer-Uhl, Liposome technology for industrial purposes. *J Drug Deliv*, 2011, 591325: 1-9.
- [17] B. Peng, P. Lloyd, H. Schran, Clinical pharmacokinetics of imatinib. *Clin Pharmacokinet*, 2005, 44(9): 879-894.
- [18] P. Ye, W. Zhang, T. Yang, et al., Folate receptor-targeted liposomes enhanced the antitumor potency of imatinib through the combination of active targeting and molecular targeting. *Int J Nanomed*, 2014, 9: 2167.
- [19] T. Wang, Y. Deng, Y. Geng, et al., Preparation of submicron unilamellar liposomes by freeze-drying double emulsions. *Biochimica et Biophysica Acta*, 2006, 1758: 222-231.
- [20] M. Kaszuba, J. Corbett, F.M. Watson, et al., High-concentration zeta potential measurements using light-scattering techniques. *Philos Trans A Math Phys Eng Sci*, 2010, 368(1927): 4439-4451.
- [21] S. Khatak, M. Mehta, R. Awasthi, et al., Solid lipid nanoparticles containing anti-tubercular drugs attenuate the *Mycobacterium marinum* infection. *Tuberculosis*, 2020, 125: 102008. doi: 10.1016/j.tube.2020.102008.
- [22] T. Guan, Y. Miao, L. Xu, et al., Injectable nimodipine-loaded nanoliposomes: preparation, lyophilization and characteristics. *Int J Pharm*, 2011, 410(1-2): 180-187.
- [23] N. Pirooznia, S. Hasannia, A.S. Lotfi, Encapsulation of alpha-1 antitrypsin in PLGA nanoparticles: *in vitro* characterization as an effective aerosol formulation in pulmonary diseases. *J Nanobiotechnology*, 2012, 10: 20.
- [24] C.M. Muller, B. Pejicic, L. Esteban, et al., Infrared attenuated total reflectance spectroscopy: an innovative strategy for analyzing mineral components in energy relevant systems. *Sci Rep*, 2014, 4: 6764.
- [25] J. Zhong, X. Yao, D.L. Li, et al., Large scale preparation of midkine antisense oligonucleotides nanoliposomes by a cross-flow injection technique combined with ultrafiltration and high-pressure extrusion procedures. *Int J Pharm*, 2013, 441(1-2): 712-720.
- [26] M. Chauhan, G. Joshi, H. Kler, et al., Dual inhibitors of epidermal growth factor receptor and topoisomerase II α derived from a quinoline scaffold. *RSC Advances*, 2016, 6: 77717-77734.
- [27] N. Solanki, M. Mehta, D.K. Chellappan, et al., Antiproliferative effects of boswellic acid-loaded chitosan nanoparticles on human lung cancer cell line A549. *Future Med Chem*, 2020, 12(22): 2019-2034. doi: 10.4155/

- fmc-2020-0083.
- [28] A. Negi, J.M. Alex, S.M. Amrutkar, et al., Imine/amide–imidazole conjugates derived from 5-amino-4-cyano-N1-substituted benzyl imidazole: microwave-assisted synthesis and anticancer activity via selective topoisomerase-II- α inhibition. *Bioorganic & Medicinal Chemistry*, 2015, 23: 5654-5661.
- [29] HiMedia product information, LA395, Dialysis Membrane-110. Available at: <http://himedialabs.com/TD/LA395.pdf>. Last accessed July 28, 2020.
- [30] A.M. Khan, F.J.Ahmad, A.K.Panda, et al., Investigation of imatinib loaded surface decorated biodegradable nanocarriers against glioblastoma cell lines: intracellular uptake and cytotoxicity studies. *Int J Pharm*, 2016, 507(1-2): 61-71.
- [31] Y. Gao, J. Zuo, N.B. Chacra, et al., *In vitro* release kinetics of antituberculosis drugs from nanoparticles assessed using a modified dissolution apparatus. *BioMed Res Int*, 2013, 2013: 136590.
- [32] N.V. Shah, A.K. Seth, R. Balaraman, et al., Nanostructured lipid carriers for oral bioavailability enhancement of raloxifene: design and *in vivo* study. *J Adv Res*, 2016, 7(3): 423-434.
- [33] L. Ramezanzade, S.F. Hosseini, M. Nikkhah, Biopolymer-coated nanoliposomes as carriers of rainbow trout skin-derived antioxidant peptides. *Food Chem*, 2017, 234: 220-229.
- [34] T.I. Shalaby, W.M.El-Refai, Bioadhesive chitosan-coated cationic nanoliposomes with improved insulin encapsulation and prolonged oral hypoglycemic effect in diabetic mice. *J Pharm Sci.*, 2018, 107(8): 2136-2143.
- [35] I.S. Chandran, P.M. Prasanna, Drug-excipient interaction studies of loperamide loaded in polysorbate 80 liposomes. *Orient J Chem*, 2015, 31(4): 2201-2206.

Copyright© Mandeep Dahiya, Rajendra Awasthi, Gaurav Gupta, Sachin Kumar Singh, Monica Gulati, Niraj Kumar Jha, Saurabh Kumar Jha, Ankur Sharma, Parteek Prasher, Krishnan Anand, Dinesh Kumar Chellappan, Kamal Dua, and Harish Dureja. This is an open-access article distributed under the terms of the Creative Commons Attribution License, which permits unrestricted use, distribution, and reproduction in any medium, provided the original author and source are credited.